

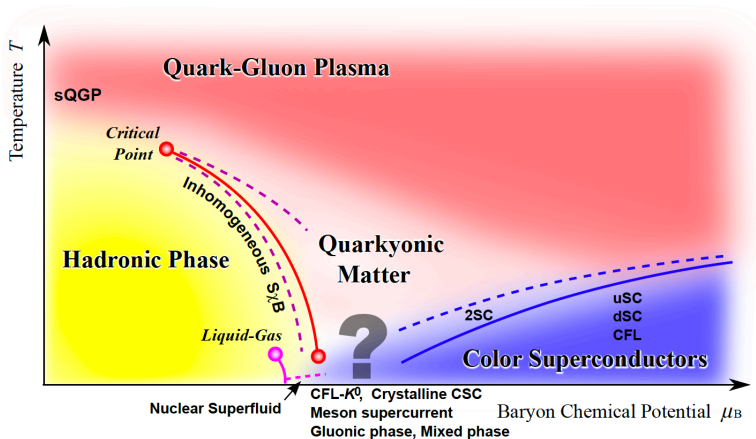
# **Complex Langevin for Complex Actions**

## Recent Developments

TIFR Free Meson Seminar,  
Thursday, October 22, 2020  
Dr. Anosh Joseph  
IISER Mohali

# Motivation

# Motivation



QCD phase diagram. [Fukushima and Hatsuda 2010]

## Motivation

Nonperturbative determination of QCD phase diagram.

Is it possible?

At low temperature ( $T$ ) and chemical potential ( $\mu$ ) QCD is confining.

May be we could use **lattice QCD**...

At  $\mu = 0$  and  $T \geq 0$  lattice QCD works well.

## Motivation

Lattice QCD is based on **importance sampling**.

Markov chain Monte Carlo (MCMC).

But when  $\mu > 0$  importance sampling breaks down.

Consider the field theory partition function

$$\begin{aligned} Z &= \int DU D\bar{\psi} D\psi e^{-S[U, \psi, \bar{\psi}]} \\ &= \int DU e^{-S_B} \det M. \end{aligned} \tag{1}$$

The term  $e^{-S_B} \det M$  can be interpreted as a **probability weight**, if  $> 0$ .

## Motivation

Then we can evaluate the above integral using importance sampling.

But for QCD at finite baryon/quark chemical potential, the **fermion determinant is complex!**

$$(\det M(\mu))^* = \det M(-\mu^*) \in \mathbb{C}. \quad (2)$$

Theory has a **sign problem**. (Complex phase problem to be more accurate.)

Importance sampling is not possible!

## Sign Problem

Can express  $\det M$  as

$$\det M = |\det M| e^{i\phi}. \quad (3)$$

Apparent solution to this complex phase problem -  
**absorb phase** in the observable

$$\begin{aligned} \langle O \rangle_{\text{full}} &= \frac{\int D U e^{-S_B} \det M O}{\int D U e^{-S_B} \det M} = \frac{\int D U e^{-S_B} |\det M| e^{i\phi} O}{\int D U e^{-S_B} |\det M| e^{i\phi}} \\ &= \frac{\langle e^{i\phi} O \rangle_{\text{pq}}}{\langle e^{i\phi} \rangle_{\text{pq}}}. \end{aligned} \quad (4)$$

## Sign Problem

Let us look at  $\langle e^{i\phi} \rangle_{\text{pq}}$ .

We have

$$\langle e^{i\phi} \rangle_{\text{pq}} = \frac{\int DU e^{-S_B} |\det M| e^{i\phi}}{\int DU e^{-S_B} |\det M|} = \frac{Z_{\text{full}}}{Z_{\text{pq}}} = e^{-\Omega \Delta f}. \quad (5)$$

$$\begin{aligned} Z_{\text{full}} &= e^{-F/T} = e^{-\Omega f} \\ Z_{\text{pq}} &= e^{-F_{\text{pq}}/T} = e^{-\Omega f_{\text{pq}}}. \end{aligned} \quad (6)$$

$\Omega$ : Spacetime volume.

$\Delta f = f - f_{\text{pq}}$ : difference in free energy densities.

$$Z_{\text{full}} \leq Z_{\text{pq}}.$$

## Sign Problem

Average phase factor goes to zero in the thermodynamic limit.

Unless  $f = f_{pq}$ .

Thus the ratio

$$\langle O \rangle_{\text{full}} = \frac{\langle e^{i\phi} O \rangle_{pq}}{\langle e^{i\phi} \rangle_{pq}} \quad (7)$$

is not well defined.

Numerator and denominator vanish exponentially as  $\Omega$  is increased.

Exponential dependence on  $\Omega \implies$  Sign problem is exponentially hard.

# Complex Langevin Method (CLM)

## Complex Langevin Method

We can resort to a method that does not use importance sampling.

Complexify all degrees of freedom

$$\phi \rightarrow \phi_R + i\phi_I. \quad (8)$$

Gives rise to enlarged complexified field space.

Could use

- (1.) **Complex Langevin** dynamics or
- (2.) **Lefschetz thimbles**.

# Complex Langevin Method

Analogy with **Brownian motion** [Parisi and Wu 1981]

A particle in a fluid experiences friction  $\alpha$  and kick  $\eta$ .

Langevin equation

$$\frac{dx(t)}{dt} = -\alpha x(t) + \eta(t), \quad (9)$$

where

$$\langle \eta(t)\eta(t') \rangle = 2\delta(t-t'). \quad (10)$$

## Complex Langevin Method

Solutions appear as that of a **stochastic process**.

Could generalize the process:  $z = x + iy$

Real Langevin  $\longrightarrow$  Complex Langevin.

There is an associated distribution  $P(x, y; t)$  in complex plane.

Complex Langevin process finds this distribution.

Importance sampling not needed.

## Complex Langevin Method

Can discretize the stochastic equation:

$$x_{n+1} = x_n + \epsilon K_n^R + \sqrt{\epsilon} \eta_n, \quad (11)$$

$$y_{n+1} = y_n + \epsilon K_n^I. \quad (12)$$

$\epsilon$ : step size.

Drift terms

$$K_n^R = -\operatorname{Re} \frac{\partial S}{\partial z} \quad \text{and} \quad K_n^I = -\operatorname{Im} \frac{\partial S}{\partial z}. \quad (13)$$

Noise satisfies

$$\langle \eta_n \eta_{n'} \rangle = 2\delta_{nn'}. \quad (14)$$

# Complex Langevin and Path Integral

Let's adapt this to field theory. [Parisi and Wu 81, Klauder 83]

$$Z = \int D\phi e^{-S[\phi]}. \quad (15)$$

Langevin dynamics happens in the “fifth” time direction

$$\frac{\partial}{\partial \tau} \phi(x, \tau) = -\frac{\delta S[\phi]}{\delta \phi(x, \tau)} + \eta(x, \tau). \quad (16)$$

$\tau$ : Langevin time.

# Complex Langevin and Path Integral

Gaussian noise

$$\begin{aligned}\langle \eta(\mathbf{x}, \tau) \rangle &= 0, \\ \langle \eta(\mathbf{x}, \tau) \eta(\mathbf{x}', \tau') \rangle &= 2\delta(\mathbf{x} - \mathbf{x}')\delta(\tau - \tau').\end{aligned}\quad (17)$$

Consider an arbitrary operator  $\mathcal{O}$  made out of field  $\phi$ .

Can define a noise averaged expectation value

$$\langle \mathcal{O}[\phi(\tau)] \rangle_{\eta} \equiv \int d\phi P[\phi(\tau)] \mathcal{O}[\phi] \quad (18)$$

## Complex Langevin and Path Integral

$P[\phi(\tau)]$ : a probability distribution.

It satisfies **Fokker-Planck equation**

$$\frac{\partial P[\phi(\tau)]}{\partial \tau} = \frac{\delta}{\delta \phi(\tau)} \left( \frac{\delta}{\delta \phi(\tau)} + \frac{\delta S[\phi]}{\delta \phi(\tau)} \right) P[\phi(\tau)]. \quad (19)$$

For real  $S$ , can show that, in the limit  $\tau \rightarrow \infty$ , stationary solution of Fokker-Planck equation

$$P[\phi] \sim e^{-S[\phi]} \quad (20)$$

will be reached.

# Complex Langevin and Path Integral

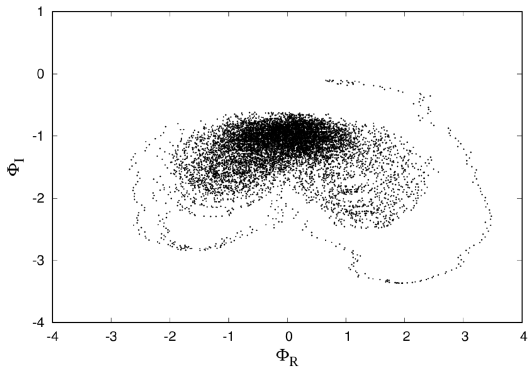
Thus guaranteeing convergence of Langevin dynamics...

... to the correct equilibrium distribution.

For complex actions there is no such proof!

But can identify if convergence works or not.

# Complex Langevin and Path Integral



[Anosh Joseph & Arpith Kumar PRD 100 (2019) 074507]

# Models with SUSY

Work done with **Arpith Kumar**

[PRD 100 (2019) 074507, arXiv:2010.nnnnn]

# Supersymmetric Quantum Mechanics

Consider a theory with complex action in 0+1 dimension.

Degrees of freedom are  $\phi$  (boson),  $\psi$  and  $\bar{\psi}$  (fermions).

Also introduce an auxiliary field  $\mathcal{B}$ .

Action has the form

$$\mathcal{S}[\phi, \psi, \bar{\psi}] = \int_0^\beta d\tau \left[ \frac{\mathcal{B}^2}{2} + i\mathcal{B} (\dot{\phi} + W'') + \bar{\psi} \left( \frac{\partial}{\partial \tau} + W'' \right) \psi \right].$$

$W \equiv W(\phi)$ : **Superpotential**.

# Supersymmetric Quantum Mechanics

Action has a symmetry - known as supersymmetry (SUSY).

Two SUSY charges:  $Q$  and  $\bar{Q}$ .

$$Q\mathcal{S} = 0, \quad \bar{Q}\mathcal{S} = 0. \quad (21)$$

Partition function in path integral formalism

$$Z = \int \mathcal{D}\phi \mathcal{D}\psi \mathcal{D}\bar{\psi} e^{-\mathcal{S}[\phi, \psi, \bar{\psi}]}. \quad (22)$$

# Lattice Regularization

Want to study this theory non-perturbatively.

Need to study **dynamical SUSY breaking**.

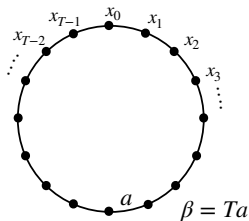
Let's put it on a lattice and simulate.

Action is complex in general.

Will use complex Langevin dynamics.

If action is real, could use Markov chain Monte Carlo (MCMC)

# Lattice Regularization



Consider a 1-d lattice  $\Lambda$ .

$T$  number of equally spaced sites, with lattice spacing  $a$ .

Physical extent:  $\beta = Ta$ .

Continuous derivatives  $\longrightarrow$  difference operators

# Lattice Regularization

Lattice action for our theory

$$\mathcal{S} = \sum_{i=0}^{T-1} \left[ \frac{1}{2} \left( \sum_{j=0}^{T-1} \nabla_{ij}^S \phi_j + \Omega'_i \right)^2 + \bar{\psi}_i \sum_{j=0}^{T-1} (\nabla_{ij}^S + \Omega''_{ij}) \psi_j \right] \quad (23)$$

$\nabla_{ij}^S$ : Symmetric difference operator.

$\Omega'_i, \Omega''_{ij}$ : Terms containing superpotential (and Wilson mass)

It respects only the  $\mathcal{Q}$  supercharge.

## Boundary Conditions

When SUSY is broken  $Z$  vanishes.

Then expectation values of observables normalized by  $Z$  could be ill-defined.

Need to overcome this difficulty.

Apply periodic boundary conditions (PBCs) for bosons and **twisted boundary conditions** (TBCs) for fermions.

Introduce a twist parameter  $\alpha$ .

Imposing TBCs is analogous to turning on an external field in the system.

## Boundary Conditions

Twisted boundary conditions

$$\phi_T = \phi_0, \quad (24a)$$

$$\psi_T = e^{i\alpha} \psi_0, \quad (24b)$$

$$\bar{\psi}_T = e^{-i\alpha} \bar{\psi}_0. \quad (24c)$$

$Z$  has the following form on lattice

$$Z_\alpha = \left( \frac{1}{\sqrt{2\pi}} \right)^T \int \left( \prod_{t=0}^{T-1} d\phi_t d\psi_t d\bar{\psi}_t \right) e^{-S_\alpha}. \quad (25)$$

## Observables

Expectation value of an observable  $\mathcal{O}$

$$\begin{aligned}\langle \mathcal{O} \rangle &= \lim_{\alpha \rightarrow 0} \langle \mathcal{O} \rangle_{\alpha} \\ &= \lim_{\alpha \rightarrow 0} \frac{1}{Z_{\alpha}} \left( \frac{1}{\sqrt{2\pi}} \right)^T \int \left( \prod_{t=0}^{T-1} d\phi_t \right) \mathcal{O} \exp \left[ -S_{\alpha}^{\text{eff}} \right].\end{aligned}$$

## Observables: Mass gaps from Correlators

Bosonic and fermionic correlation functions

$$G_{\alpha}^B(k) = \langle \phi_0 \phi_k \rangle_{\alpha}, \quad (26)$$

$$G_{\alpha}^F(k) = \langle \bar{\psi}_0 \psi_k \rangle_{\alpha}, \quad (27)$$

Mass gaps can be extracted either by a

$$\cosh \left[ ma \left( t - \frac{T}{2} \right) \right] \quad (28)$$

fit for the  $t$ -th lattice site.

Or a simple exponential fit over say, the first or last  $T/4$  time slices of the correlation functions.

## Observables: The field $\mathcal{B}$

Observable  $\mathcal{B}_\alpha$  can effectively predict SUSY breaking.

$$\lim_{\alpha \rightarrow 0} \mathcal{B}_\alpha \begin{cases} \neq 0 & \text{broken} \\ = 0 & \text{preserved.} \end{cases} \quad (29)$$

## Observables: Bosonic action

Bosonic action can also be used to see SUSY breaking

$$S_{\alpha}^B = \sum_{i=0}^{T-1} \frac{1}{2} N_i^2 = \sum_{i=0}^{T-1} \frac{1}{2} \left( \sum_{j=0}^{T-1} \nabla_{ij}^- \Phi_j + \Xi'_i \right)^2. \quad (30)$$

Expect  $\langle S \rangle = T$ , and  $\langle S^B \rangle = \frac{1}{2}T$ .

$$\lim_{\alpha \rightarrow 0} S_{\alpha}^B \begin{cases} \neq \frac{1}{2}T & \text{broken} \\ = \frac{1}{2}T & \text{preserved.} \end{cases} \quad (31)$$

## Observables: Ward Identities

Add source terms  $(J, \theta, \bar{\theta})$

$$Z_\alpha(J, \theta, \bar{\theta}) = \left(\frac{1}{\sqrt{2\pi}}\right)^T \int \left(\prod_{t=0}^{T-1} d\phi_t d\psi_t d\bar{\psi}_t\right) \times \exp \left[ -\mathcal{S}_\alpha + \sum_{t=0}^{T-1} (J_t \phi_t + \theta_t \bar{\psi}_t + \bar{\theta}_t \psi_t) \right].$$

Variation of  $Z_\alpha$  under  $\mathcal{Q}$ -transformations vanishes upon turning off the external sources.

$$\mathcal{Q}Z_\alpha(J, \theta, \bar{\theta}) \Big|_{\text{sources}=0} = 0. \quad (32)$$

## Observables: Ward Identities

We have

$$\begin{aligned} \Omega \left[ \frac{\partial^2 Z}{\partial J_j \partial \theta_i} \right] &= 0 \\ \implies \langle \bar{\Psi}_i \Psi_j \rangle + \langle N_i \phi_j \rangle &= 0. \end{aligned}$$

$$N_i = \sum_{j=0}^{T-1} \nabla_{ij}^S \phi_j + \Omega'_i.$$

Can use this **Ward Identity** to investigate spontaneous SUSY breaking.

## Simulations: Double-Well Potential

Consider the potential

$$W'(\phi) = g \left( \phi^2 + \mu^2 \right).$$

SUSY is broken in this model [Witten 1981].

We also consider a complexified double-well potential

$$W'(\phi) = ig \left( \phi^2 + \mu^2 \right).$$

# Simulations: Real Double-Well Potential

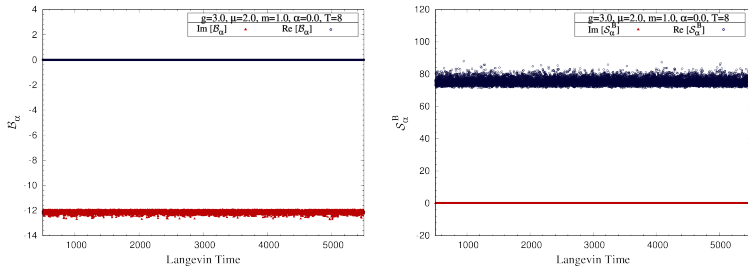


Figure:  $\mathcal{B}_\alpha$  (Left) and  $\mathcal{S}_\alpha^B$  (Right). Real double-well potential.

SUSY is broken in this model.

$\mathcal{B}_\alpha$  does not fluctuate around 0. Also,  $\mathcal{S}_\alpha^B \neq \frac{1}{2}T$ .

# Simulations: Complex Double-Well Potential

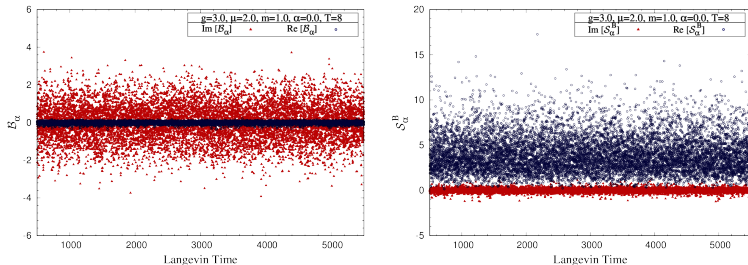


Figure:  $B_\alpha$  (Left) and  $S_\alpha^B$  (Right). Complex double-well potential.

SUSY is unbroken in this model.

$B_\alpha$  fluctuates around 0.  $S_\alpha^B$  fluctuates around  $\frac{1}{2}T = 4$

# Simulations: Ward Identities

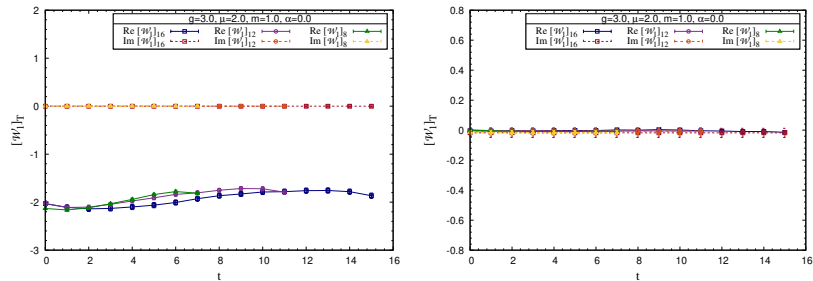


Figure: Ward identities. (Left) real and (Right) complex double-well superpotentials.

## Simulations: Models with $\mathcal{PT}$ Symmetry

Superpotential

$$W'(\phi) = -ig (i\phi)^{(1+\delta)} \quad (33)$$

$\delta$ : a continuous parameter.

SUSY Lagrangian for this model breaks  $\mathcal{P}$  symmetry.

Would be interesting to ask if breaking of  $\mathcal{P}$  induces a breaking of SUSY.

Explored using perturbation theory in **Bender 1997**.

## Simulations: Models with $\mathcal{PT}$ Symmetry

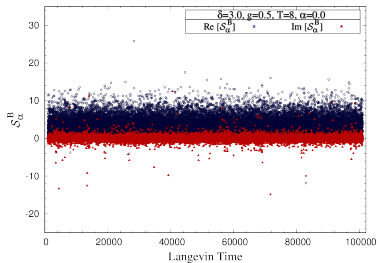
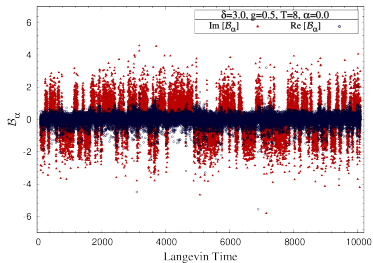
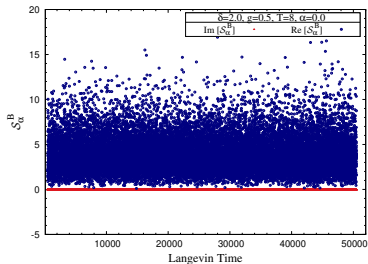
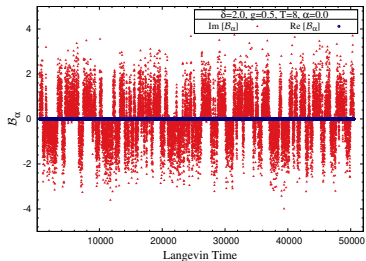
Perturbative analysis (in  $\delta$ ) showed that SUSY is unbroken.

Let's explore SUSY breaking in this model (in 1-d) using CLM.

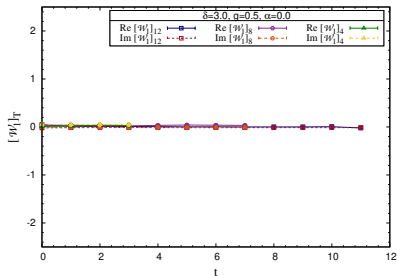
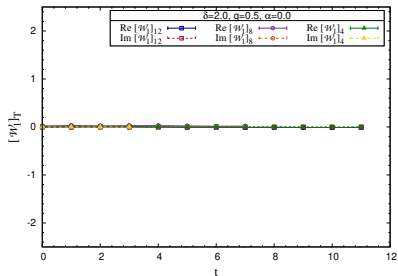
Note that path integral Monte Carlo fails here.

Since action of this model can be complex, in general.

# Simulations: Models with $\mathcal{PT}$ Symmetry



# Simulations: Ward Identities



# Reliability of CLM

How to check if our simulations are reliable?

Correctness criteria:

- (1.) Can use **Fokker-Planck equation**.
- (2.) **Decay of the drift term**.

## Correctness Criterion: Fokker-Planck Equation

Holomorphic observables of the theory  $\mathcal{O}_k[\phi, \tau]$  at  $k$ -th lattice site evolve in the following way

$$\frac{\partial \mathcal{O}_k[\phi, \tau]}{\partial \tau} = \tilde{L}_k \mathcal{O}_k[\phi, \tau]. \quad (34)$$

$\tilde{L}_k$ : **Langevin operator** for  $k$ -th site

$$\tilde{L}_k = \left( \frac{\partial}{\partial \phi_k} - \frac{\partial \mathcal{S}[\phi]}{\partial \phi_k} \right) \frac{\partial}{\partial \phi_k}. \quad (35)$$

## Correctness Criterion: Fokker-Planck Equation

Once the equilibrium distribution is reached we should have

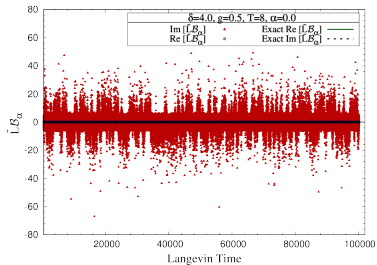
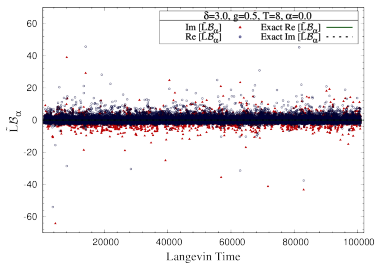
$$C_{\mathcal{O}_k} \equiv \langle \tilde{L}_k \mathcal{O}_k[\phi] \rangle = 0. \quad (36)$$

This can be used as a criterion for correctness of the complex Langevin method.

Take the auxiliary field  $\mathcal{B}_k$  at  $k$ -th site as the observable  $\mathcal{O}_k$

$$\tilde{L}_k \mathcal{O}_k = \tilde{L}_k \mathcal{B}_k. \quad (37)$$

# Correctness Criterion: Fokker-Planck Equation



$\tilde{L}_\alpha$  fluctuates around 0.

## Correctness Criterion: Decay of Drift Terms

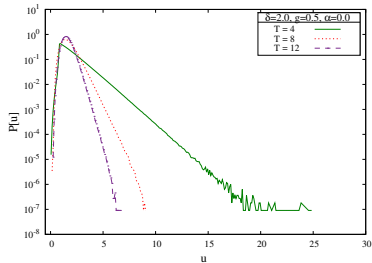
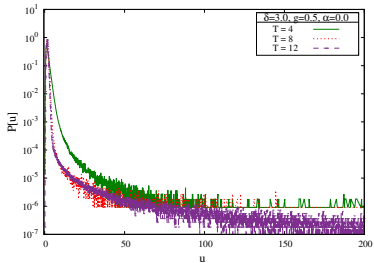
Another test to check correctness.

Look at probability distribution  $P(u)$  of the magnitude of the drift term  $u$

$$u = \sqrt{\frac{1}{T} \sum_{k=0}^{T-1} \left| \frac{\partial \mathcal{S}^{\text{eff}}}{\partial \phi_k} \right|^2}.$$

Probability of drift term **should be suppressed exponentially** at larger magnitudes in order to guarantee the correctness of CLM.

# Correctness Criterion: Decay of Drift Terms



# Complex Unitary Matrix Model

Work done with **Pallab Basu** and **Kasi Jaswin**  
[Phys. Rev. D 98 (2018) 3, 034501]

# Complex Unitary Matrix Model

A unitary matrix model arises in a **one-loop formulation of QCD** on compact spaces

Often  $S^1 \times S^3$

Analogous to  $SU(N)$  gauge theories.

Originally derived by **Sundborg** 1999, **Aharony** 2003, **Alvarez-Gaume** 2005...

... for theories with more general matter content.

## Complex Unitary Matrix Model

One-loop effective action of QCD on  $S^1 \times S^3$  with  $\beta = T^{-1}$ , chemical potential  $\mu$  and quark mass  $m$

$$\begin{aligned} S = & \sum_{n=1}^{\infty} \frac{1}{n} z_b \left( \frac{n\beta}{R} \right) \text{Tr } U^n \text{Tr } U^{\dagger n} \\ & + \sum_{n=1}^{\infty} \frac{(-1)^n}{n} N_f z_f \left( \frac{n\beta}{R}, mR \right) \\ & \times \left[ e^{n\beta\mu} \text{Tr } U^n + e^{-n\beta\mu} \text{Tr } U^{\dagger n} \right]. \quad (38) \end{aligned}$$

$R$ : radius of  $S^3$ ,  $N_f$ : number of flavors of **fundamental fermions**.

Model has a tower of quark energy levels due to compactification.

# Complex Unitary Matrix Model

Quadratic term in Polyakov loop - contribution from adjoint fields

Linear term - contribution from the fundamental matter fields.

Adjoint contribution taken as bosonic.

Contribution from fundamental fields taken as fermionic.

## Complex Unitary Matrix Model

In the low temperature limit,  $\beta \rightarrow \infty$

$$z_b(\infty) = 0. \quad (39)$$

So the gluonic contribution is negligible.

Thus the action is

$$S = S_{\text{Vdm}} + S_f. \quad (40)$$

$S_{\text{Vdm}}$ : Vandermonde piece of the action

$S_f$ : fundamental fermionic contribution.

## Complex Unitary Matrix Model

Fermionic part could be summed in a logarithm

$$S[U] = - \sum_{l=1}^{\infty} \sigma_l \left( \log \left[ \det \left( 1 + e^{\beta(\mu - \epsilon_l)} U \right) \right. \right. \\ \left. \left. \times \det \left( 1 + e^{\beta(-\mu - \epsilon_l)} U^{-1} \right) \right] \right). \quad (41)$$

$$\sigma_l = 2l(l+1) \frac{N_f}{N}, \quad (42)$$

$$\epsilon_l = \sqrt{m^2 + \left( l + \frac{1}{2} \right)^2 R^{-2}}. \quad (43)$$

## Observables

**Polyakov loop** and its inverse:  $P$  and  $P^{-1}$

Can use these to study confined/deconfined phases.

**Fermion number**  $f_N$

It gives the number of fermions minus the number of anti-fermions in a given volume

$$f_N = \frac{1}{\beta} \left( \frac{\partial \log Z}{\partial \mu} \right). \quad (44)$$

## Observables

### Quark number susceptibility

$$\chi_f = \frac{1}{\beta} \frac{\partial f_N}{\partial \mu}. \quad (45)$$

Serves as an indicator of confinement/deconfinement transitions for nonzero  $\mu$ .

**Pressure:**  $p = \frac{1}{\beta} \left( \frac{\partial \log Z}{\partial V_3} \right)$

$V_3$ : spatial volume.

**Energy  $E$ :** Can be constructed from pressure and fermion number density

$$E = -pV_3 + \mu f_N. \quad (46)$$

## Single Level Model

Truncate action in Eq. (59) in a double scaling limit:

$$\beta \rightarrow \infty, \quad \mu \rightarrow \epsilon_0$$

$\epsilon_0$ : a fixed quark energy level

Only contribution from a single level survives

Define a transition parameter

$$\xi \equiv e^{(\beta(\mu - \epsilon_l))}. \quad (47)$$

Action takes the form

$$S[U] = -\sigma \log(1 + \xi U). \quad (48)$$

## Single Level Model

Effective action on the complexified angle variables includes Vandermonde piece and a Lagrange multiplier.

In the large  $N$  limit, the integral over the angles is dominated by a saddle point

$$\frac{\partial S}{\partial \theta_i} = iN\mathcal{N} - \frac{iN\sigma\xi e^{i\theta}}{(1 + \xi e^{i\theta_i})} - \sum_{j(\neq i)}^N \cot\left(\frac{\theta_i - \theta_j}{2}\right). \quad (49)$$

Note that the action is not Hermitian.

Gives rise to the *sign problem* in the presence of a chemical potential.

## Single Level Model

As a result, the saddle point configuration will lie out in the complex plane.

Let us look at the various regimes of  $\xi$ .

And see how it affects the eigenvalue distribution.

Analytical study is given in **Hands 2010**.

# Single Level Model

*Small  $\xi$ , confined phase*

Effective fermion number vanishes,  $\mathcal{N} = 0$ .

We also have

$$P = 0, \quad P^{-1} = \sigma\xi. \quad (50)$$

Note that  $P \neq P^{-1}$  - a feature of the complex action.

## Single Level Model

As  $\xi$  is increased the contour of eigenvalue distribution opens into an arc,...

... just as the matrix model solved by **Gross** and **Witten** [Gross (1980)] and **Wadia** [Wadia (1980)].

Line of phase transitions in the  $(\mu, T)$  plane corresponds to the straight line

$$\mu = \epsilon - T \left[ (1 + \sigma) \log(1 + \sigma) - \sigma \log \sigma \right]. \quad (51)$$

Above approximation valid only in the  $(\beta \rightarrow \infty)$  limit.

## Single Level Model

*Large  $\xi$  confined phase*

Effective fermion number is

$$\mathcal{N} = \sigma. \quad (52)$$

Indicates that the level is now occupied.

Polyakov line expectation values are

$$P = \frac{\sigma}{\xi}, \quad P^{-1} = 0. \quad (53)$$

## Single Level Model

Comparing with the previous case: behavior of  $P$  and  $P^{-1}$  swaps over along the replacement  $\xi \rightarrow \xi^{-1}$ .

Large  $\xi$  confined phase persists until the value

$$\xi = \xi_2 = \frac{(1 + \sigma)^{1+\sigma}}{\sigma^\sigma}. \quad (54)$$

For smaller values of  $\xi$  the contour of eigenvalue distribution is not closed and the phase does not exist.

## Single Level Model

Points of transition  $\xi = \xi_1$  and  $\xi = \xi_2$  satisfy

$$\xi_1 \xi_2 = 1. \quad (55)$$

In the  $(\mu, T)$  plane, the boundary lies along the straight line

$$\mu = \epsilon + T \left[ (1 + \sigma) \log(1 + \sigma) - \sigma \log \sigma \right]. \quad (56)$$

Again valid in the low temperature limit.

## Single Level Model

### *Deconfined phase*

In the region  $\xi_1 \leq \xi \leq \xi_2$ , experience with GWW matrix model suggests that the eigenvalue distribution exhibits the shape of an open contour.

In this regime, we get a condition (Hands 2010)

$$\xi = \frac{(\sigma - \mathcal{N})^{\sigma - \mathcal{N}} (1 + \mathcal{N})^{1 + \mathcal{N}}}{\mathcal{N}^{\mathcal{N}} (1 + \sigma - \mathcal{N})^{1 + \sigma - \mathcal{N}}}. \quad (57)$$

This equation determines  $\mathcal{N}$  as a function of  $\xi$ .

## Single Level Model

From the above equation, it follows that across the transitions at  $\xi = \xi_1$  and  $\xi = \xi_2$ ,  $\mathcal{N}$  and its first derivative  $\partial\mathcal{N}/\partial\mu$  are continuous.

However higher derivatives are discontinuous.

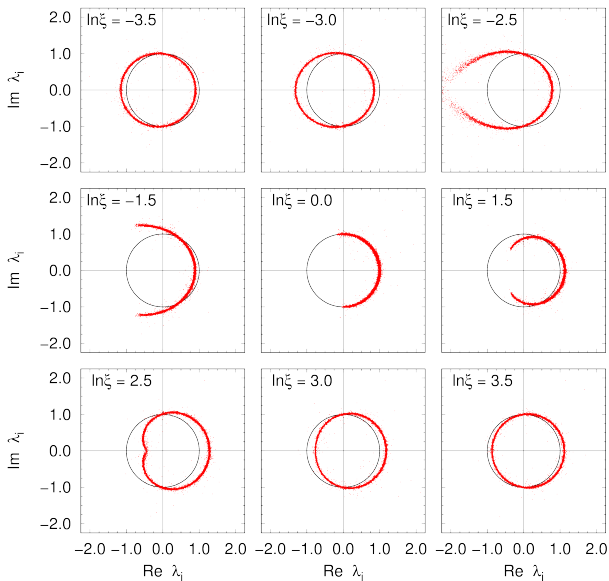
Since  $\mathcal{N}$  is the effective fermion number, the first derivative of the grand potential, it follows that the **transitions are third order**,...

... just as in the original **GWW model**.

For a single winding we have

$$P = \frac{\mathcal{N}}{\sigma + 1 - \mathcal{N}} \frac{1}{\xi}, \quad P^{-1} = \frac{\sigma - \mathcal{N}}{1 + \mathcal{N}} \xi. \quad (58)$$

# Single Level Model



## Single Level Model

Figure above: Eigenvalue distributions in the confined/deconfined phases as a function of  $\log \xi$  for the single level matrix model with positive  $\mu$ .

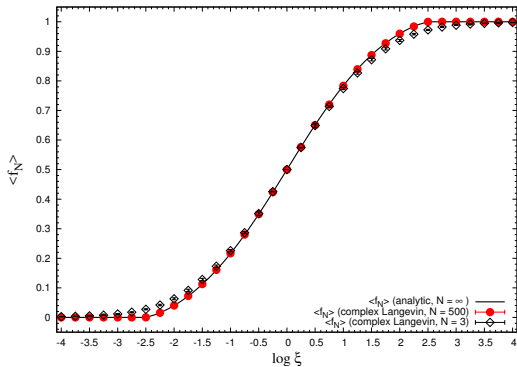
Form of the action is given in Eq. (48).

$N = N_f = 500$ , and quark mass  $m = 0$ .

Data are obtained through CLM with adaptive Langevin step sizes  $\Delta\tau \leq 0.00005$ ,  $N_{\text{therm}} = 18000$ ,  $N_{\text{gen}} = 2000$  and with measurements performed with an interval of 100 steps.

The solid unit circles are guide to the eye.

# Single Level Model



## Single Level Model

Figure above: Effective fermion number  $\langle f_N \rangle$  across the pair of GWW transitions from the small  $\xi$  confined phase through the deconfined phase to the large  $\xi$  confined phase for the single level model with positive  $\mu$ .

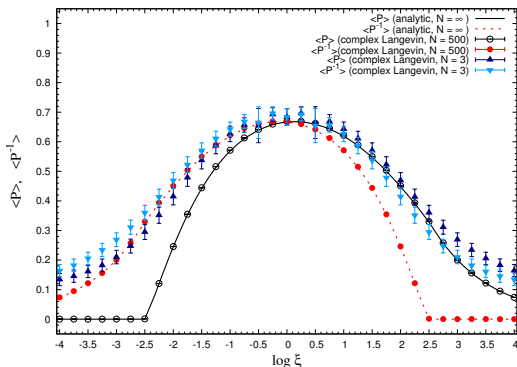
Form of the action given in Eq. (48).

Simulation data are for quark mass  $m = 0$ ,  $N = N_f = 500$  and  $N = N_f = 3$ .

Solid curve is the analytical result ( $N = \infty$ ).

We used adaptive Langevin step sizes  $\Delta\tau \leq 0.00005$ ,  $N_{\text{therm}} = 10000$ ,  $N_{\text{gen}} = 10000$  and measurements are performed with an interval of 100 steps.

# Single Level Model



$\langle P \rangle$  and  $\langle P^{-1} \rangle$  across a pair of GWW transitions from the small  $\xi$  confined phase through the deconfined phase to the large  $\xi$  confined phase.

## Single Level Model

Figure above:

Single level model with positive  $\mu$ .

Transitions from confined/deconfined phases occur when either  $\langle P \rangle$  or  $\langle P^{-1} \rangle$  vanish.

Solid and dotted curves: analytical results ( $N = \infty$ ).

Data are for quark mass  $m = 0$ ,  $N = N_f = 500$  and  $N = N_f = 3$ .

## Silver Blaze Problem

Consider a particle with mass  $m$  and a conserved charge at low  $T$ .

Can consider  $\mu$  as the change in free energy when a particle carrying the conserved charge is added.

That is, the energy cost for adding one particle.

If  $\mu < m$ : not enough energy available to create a particle  
 $\implies$  no change in the ground state.

If  $\mu > m$ : plenty of energy available  $\implies$  the ground state has a nonzero density of particles.

## Silver Blaze Problem

Statistical mechanics tells us that at zero temperature the density becomes nonzero (the 'onset') at  $\mu = \mu_c = m$ .

At strictly zero temperature, we note therefore that thermodynamic quantities...

(free energy, pressure, fermion number, susceptibility, ...)

...are independent of  $\mu$  when  $\mu < \mu_c$ ...

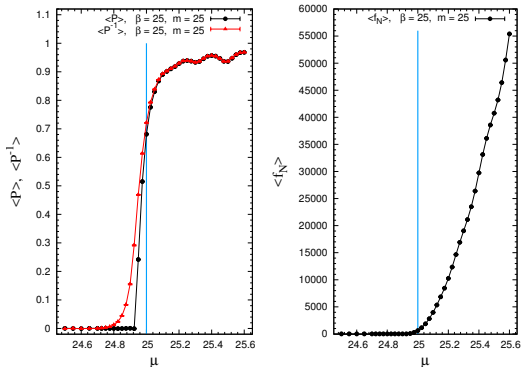
As long as  $\mu$  is below the mass of the lightest particle in the channel with the appropriate quantum numbers.

## Silver Blaze Problem

How this independence emerges in numerical simulations is nontrivial...

Has been dubbed the *Silver Blaze problem*.

# Single Level Model



Silver Blaze behavior of  $\langle P \rangle$  and  $\langle P^{-1} \rangle$ , and  $\langle f_N \rangle$  at non-zero quark mass  $m$  for the model given by the action in Eq. (59).

# Single Level Model

Onset at  $\mu = m = 25$ .

Marked by the solid vertical lines in the figures.

Here  $N = N_f = 500$  and  $\beta = 25$  (low  $T$ ).

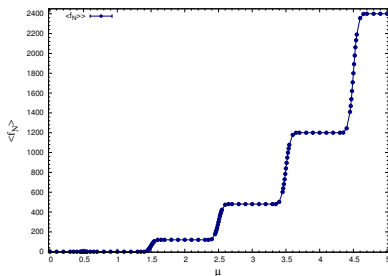
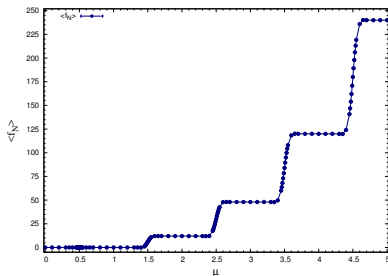
# QCD on $S^1 \times S^3$ at Finite $\mu$

Can simulate the model for  $N = 3$ .

Form of the action is the same as Eq. (59)

$$S[U] = - \sum_{l=1}^{\infty} \sigma_l \left( \log \left[ \det \left( 1 + e^{\beta(\mu - \epsilon_l)} U \right) \right. \right. \\ \left. \left. \times \det \left( 1 + e^{\beta(-\mu - \epsilon_l)} U^{-1} \right) \right] \right). \quad (59)$$

# QCD on $S^1 \times S^3$ at Finite $\mu$



Fermion number  $\langle f_N \rangle$  as a function of  $\mu$  for  $m = 0$  and  $\beta = T^{-1} = 30$  (low temperature).

(Left)  $N = N_f = 3$  and (Right)  $N = N_f = 30$ .

## QCD on $S^1 \times S^3$ at Finite $\mu$

Presence of an **occupation level structure** is evident.

Transitions occur when  $\epsilon_l - \mu$  changes sign.

That is, when  $\mu$  passes a quark energy level.

$\langle f_N \rangle$  can be used as an order parameter of the confinement/deconfinement transitions in the large  $N$  theory.

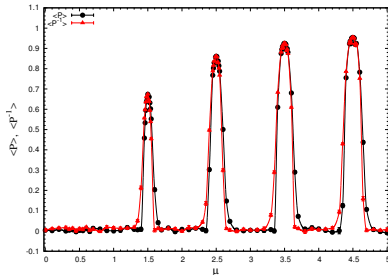
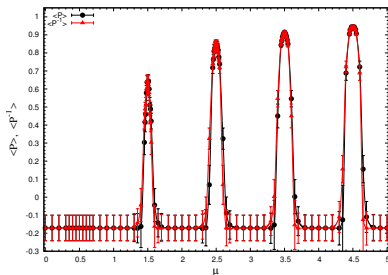
## QCD on $S^1 \times S^3$ at Finite $\mu$

First and second derivatives of the grand potential,  $\langle f_N \rangle$  and  $\langle \partial f_N / \partial \mu \rangle$  are continuous as a function of  $\mu$ .

But the third derivative  $\langle \partial^2 f_N / \partial \mu^2 \rangle$  is discontinuous.

Indicates that the transitions are third order, of the **GWW type**.

# QCD on $S^1 \times S^3$ at Finite $\mu$



Expectation values of  $\langle P \rangle$  and  $\langle P^{-1} \rangle$  as a function of  $\mu$  for QCD on  $S^1 \times S^3$ .

Here  $m = 0$ , inverse temperature  $\beta = 30$ ,  $N = N_f = 3$  (Left) and  $N = N_f = 30$  (Right).

Solid lines are to guide the eye.

## QCD on $S^1 \times S^3$ at Finite $\mu$

When  $\mu = 0$ ,  $\langle P \rangle$  and  $\langle P^{-1} \rangle$  coincide.

Each spike in  $\langle P \rangle$  and  $\langle P^{-1} \rangle$  corresponds to a level transition in  $\langle f_N \rangle$ .

The behavior of  $\langle P^{-1} \rangle$  always precedes that of  $\langle P \rangle$  at the start and finish of each level transition.

Lines peak at  $\mu = 1.5, 2.5, \dots$ .

Widths of deconfined regions increase as  $\mu$  is increased.

## Conclusions

- ▶ Complex Langevin sounds promising.
- ▶ Works well for lower dimensional theories.
- ▶ Can be used for models relevant for **superstring theory, AdS/CFT** (Nishimura 2018, 2019).
- ▶ Real test - **QCD** with finite baryon/quark chemical potential in 4d.

End